A Synchronization-Free Approach to Data Recovery for Multiple Access UWB Communications

*Vincenzo Lottici**, *Zhi Tian*† and *Geert Leus*‡

*Department of Information Engineering, University of Pisa, Pisa, Italy
†Dept. of Electrical & Computer Engineering, Michigan Technological University, Houghton, MI, USA
‡Faculty of Electrical Engineering, Delft University of Technology, Delft, The Netherlands
Emails: vincenzo.lottici@iet.unipi.it; ztian@mtu.edu; g.leus@tudelft.nl

***Abstract*— Ultra-wideband (UWB) wireless channels provide very large diversity, but make the receiver design a demanding task as far as channel estimation and timing recovery are concerned. This paper contributes with a novel receiver structure based on the multiple symbols differential detection (MSDD) framework, which bypasses not only costly channel estimation but also relaxes the stringent requirements imposed on timing recovery. Simulation results carried out in typical dense multipath propagation scenarios verify that appealing detection performance is achieved at affordable complexity thanks to an efficient implementation based on the sphere decoding (SD) algorithm.**

I. Introduction

Conveying information over a stream of very low power density and ultrashort pulses, the UWB concept lends itself to efficiently meeting the stringent requirements of state-of-the-art low-cost short-range high-speed wireless communications, offering many appealing features, such as fine timing resolution, robustness against multipath, potentiality for very high data rates and large user capacity, and coexistence with existing services via frequency-overlay operations [1]. The harsh multipath propagation conditions occurring in indoor environments, however, make the energy capture of the received waveform a very demanding task, especially in view of the limited receiver affordable complexity. The well-known Rake receiver has the potential of capturing a significant level of received energy, but the cost to be paid that inhibits its choice is a large number of correlator-based fingers together with an intensive computational load involved in the estimation of channel parameters [2]. Viable alternative approaches for efficient energy capture without requiring any prior channel estimation have been recently proposed in the form of transmitted reference (TR) methods or differential detectors (DDs) [3]-[4]. The inherent drawbacks still being present in the above approaches, such as additional transmit power and decreased data rate caused by the reference pulses in TR and poor performance for multiple access environments in DD, have been recently circumvented with the introduction of the multiple symbol differential detection (MSDD) scheme, as pursued in [5]. Herein, the channel invariance within the coherence time is exploited to jointly detect a block of differentially-encoded symbols experiencing the same unknown channel, without any knowledge of the multipath channel impulse response. The MSDD enables promising energy-efficient receivers in comparison with traditional processing schemes, but the condition to be fulfilled is that accurate timing information be recovered from the received signal.

This paper contributes to deriving a novel receiver structure based on the MSDD framework under the assumption that timing information is only partially acquired with a rough accuracy within the symbol interval. Following the GLRT rule as optimization criterion, the strategy we end up leads to a novel multi-symbol detection scheme, in the sequel referred to as synchronization-free MSDD or SF-MSDD for short, that requires the *economical* information where the symbol boundaries are roughly located, rather than *costly* timing synchronization at frame or even at pulse level. Simulation results are provided to corroborate the effectiveness of the proposed scheme in achieving considerable detection performance in typical multipath indoor propagation environments.

II. System Model

In UWB impulse radio signaling, each symbol is conveyed over a block of N_f frames with one pulse $p(t)$ per frame. The symbol, frame and pulse durations are denoted as T_s, T_f and T_p respectively, satisfying $T_s = N_f T_f$, $T_f \gg T_p$, and T_p being on the order of (sub-)nanoseconds. Concurrent channel access is enabled by employing user user-specific pseudo-random time hopping (TH) codes $\{c_j\}_{j=0}^{N_f-1} \in [0, N_c - 1]$, that time-shift pulse positions at multiples of the chip period T_c, with $N_c T_c < T_f$. Differentially encoding the independent

978-1-4244-1827-5/08/$25.00

information-bearing symbols $a_i \in \{\pm 1\}$ into the channel symbols $b_i \in \{\pm 1\}$ through the rule $b_i = a_i b_{i-1}$, and defining $u_s(t) = \sum_{j=0}^{N_f-1} u(t - jT_f - c_j T_c)$ the received symbol-level waveform with non-zero support less than T_s (i.e., ISI-free condition is satisfied), the received signal in the interval $0 \le t \le (M+1)T_s$ at the output a slow-fading multipath channel (assumed to be time-invariant within each block) can be written as

$$y(t) = \sum_{i=0}^{M} b_i u_s(t - iT_s - \tau) + w(t), \qquad (1)$$

where τ is the timing offset, $u(t) = \sum_{l=0}^{L-1} \alpha_l p(t - \tau_l)$ of width T_u, L is the total number of channel paths, each with gain α_l and delay τ_l, whereas the additive noise $w(t)$ accounts for the contribution of both the thermal noise and MAI.

III. Synchronization-Free Multiple Symbol Differential Detection

In this section, we derive the structure of a novel MSDD scheme whose aim is to recover M consecutive differentially-encoded information symbols $\mathbf{a} \triangleq [a_1, a_2, \cdots, a_M]^T$ from the received signal $y(t)$ in the interval $0 \le t \le (M+1)T_s$. The following main assumptions are adopted: *i)* timing synchronization is acquired just at symbol level, i.e., the timing offset τ is assumed to be within the interval $[0, T_s)$; *ii)* the data block size $(M+1)T_s$ is smaller than the channel coherence time so that hereinto the channel is considered as being time-invariant; *iii)* the channel impulse response is unknown and will not be explicitly estimated during detection in order to reduce the overall receiver complexity; *iv)* the composite noise $w(t)$, including both ambient noise and MAI, is modeled as a wide sense stationary white Gaussian process with two-sided power spectral density $\mathcal{N}_0/2$.

To point up the rationale of our synchronization-Free MSDD algorithm, let us partition the received symbol-level waveform $u_s(t)$ into the two segments

$$u_s^{(0)}(t) \triangleq \begin{cases} 0, & t \in [0, \tau) \\ u_s(t - \tau), & t \in [\tau, T_s) \end{cases}, \qquad (2)$$

$$u_s^{(1)}(t) \triangleq \begin{cases} u_s(t + T_s - \tau), & t \in [0, \tau) \\ 0, & t \in [\tau, T_s) \end{cases}, \qquad (3)$$

both of which rely on the unknown timing offset τ. Thus, making use of (2)-(3) and expressing the differentially-encoded channel symbol as $b_i = b_0 \prod_{k=1}^{i} a_k$, $i > 0$, the received signal (1) can be put in the alternative form

$$y(t) = \sum_{i=0}^{M} \prod_{k=0}^{i} a_k q(t - iT_s) + \sum_{i=1}^{M+1} \prod_{k=0}^{i-1} a_k g(t - iT_s) + w(t), \qquad (4)$$

where $q(t) \triangleq b_0 u_s^{(0)}(t)$ and $g(t) \triangleq b_0 u_s^{(1)}(t)$ with non-zero support T_s contain the channel parameters, the timing offset and the initial channel symbol b_0. Now, the fact that $q(t)$ and $g(t)$ are both unknown to the receiver suggests to detect the information symbols $\mathbf{a}$ following the GLRT rule. This means maximizing the log-likelihood metric (LLM)

$$\Lambda\left[y(t)\,|\tilde{\mathbf{a}}, \tilde{q}(t), \tilde{g}(t)\right] = 2\int_0^{(M+1)T_s} y(t)\tilde{s}(t)dt - \int_0^{(M+1)T_s} \tilde{s}^2(t)dt \qquad (5)$$

over $\tilde{\mathbf{a}} = [\tilde{a}_1, \tilde{a}_2, \cdots, \tilde{a}_M]^T$ and all the finite-energy functions $\tilde{q}(t)$ and $\tilde{g}(t)$ with support in $[0, T_s]$, where

$$\tilde{s}(t) = \sum_{i=0}^{M} \prod_{k=0}^{i} \tilde{a}_k \tilde{q}(t - iT_s) + \sum_{i=1}^{M+1} \prod_{k=0}^{i-1} \tilde{a}_k \tilde{g}(t - iT_s) \qquad (6)$$

is the signal corresponding to the trial values $\tilde{\mathbf{a}}$, $\tilde{q}(t)$ and $\tilde{g}(t)$. Substituting (6) into (5), the LLM takes the form

$$\Lambda\left[y(t)\,|\tilde{\mathbf{a}}, \tilde{q}(t), \tilde{g}(t)\right] = 2\int_0^{T_s} \left[\tilde{q}(t) z_1(t;\tilde{\mathbf{a}}) + \tilde{g}(t) z_2(t;\tilde{\mathbf{a}})\right] dt - \int_0^{T_s} \left[\tilde{q}^2(t) + \tilde{g}^2(t)\right] dt - 2\eta(\tilde{\mathbf{a}}) \int_0^{T_s} \tilde{q}(t)\tilde{g}(t)dt, \qquad (7)$$

where

$$z_1(t;\tilde{\mathbf{a}}) \triangleq \frac{1}{M+1} \sum_{i=0}^{M} \prod_{k=0}^{i} \tilde{a}_k y(t + iT_s), t \in \mathcal{I}_s, \qquad (8)$$

$$z_2(t;\tilde{\mathbf{a}}) \triangleq \frac{1}{M+1} \sum_{i=1}^{M+1} \prod_{k=0}^{i-1} \tilde{a}_k y(t + iT_s), t \in \mathcal{I}_s, \qquad (9)$$

$\mathcal{I}_s \triangleq [0, T_s)$ is the symbol interval and $\eta(\tilde{\mathbf{a}}) \triangleq \frac{1}{M+1} \sum_{i=1}^{M} \tilde{a}_i$. The GLRT-based decision strategy on the information symbols $\mathbf{a}$ can thus be formulated as

$$\hat{\mathbf{a}} = \arg\max_{\tilde{\mathbf{a}}} \left\{ \max_{\tilde{q}(t), \tilde{g}(t)} \left\{ \Lambda\left[y(t)\,|\tilde{\mathbf{a}}, \tilde{q}(t), \tilde{g}(t)\right] \right\} \right\}. \qquad (10)$$

In order to solve (10), we first keep $\tilde{\mathbf{a}}$ fixed and compute the inner term

$$\Gamma\left[y(t)\,|\tilde{\mathbf{a}}\right] \triangleq \max_{\tilde{q}(t), \tilde{g}(t)} \left\{ \Lambda\left[y(t)\,|\tilde{\mathbf{a}}, \tilde{q}(t), \tilde{g}(t)\right] \right\}. \qquad (11)$$

To this end, we can resort to standard variational techniques by letting $\tilde{q}(t) = q_0(t)+\lambda\varepsilon(t)$ and $\tilde{g}(t) = g_0(t)+\mu\rho(t)$, $q_0(t)$ and $g_0(t)$ being the optimum solutions to be found, and $\varepsilon(t)$ and $\rho(t)$ two generic functions with support in $\mathcal{I}_s$. After taking the first-order derivatives of $\Lambda\left[y(t)\,|\tilde{\mathbf{a}}, \tilde{q}(t), \tilde{g}(t)\right]$ with respect to λ and μ and setting them to zero, we get

$$q_0(t) = \frac{z_1(t;\tilde{\mathbf{a}}) - \eta(\tilde{\mathbf{a}})z_2(t;\tilde{\mathbf{a}})}{1-\eta^2(\tilde{\mathbf{a}})}, \tag{12}$$

$$g_0(t) = \frac{z_2(t;\tilde{\mathbf{a}}) - \eta(\tilde{\mathbf{a}})z_1(t;\tilde{\mathbf{a}})}{1-\eta^2(\tilde{\mathbf{a}})}. \tag{13}$$

Using (12)-(13) into (7), through (8)-(9) (11) can be put in the alternative form (up to an irrelevant multiplicative factor)

$$\Gamma\left[y(t)\,|\tilde{\mathbf{a}}\right] = \int_0^{T_s} \left[z_1^2(t;\tilde{\mathbf{a}}) + z_2^2(t;\tilde{\mathbf{a}}) - 2\eta(\tilde{\mathbf{a}})z_1(t;\tilde{\mathbf{a}})z_2(t;\tilde{\mathbf{a}})\right] dt, \tag{14}$$

Therefore, according to (10), the SF-MSDD detection rule reads as

$$\hat{\mathbf{a}} = \arg\max_{\tilde{\mathbf{a}}} \left\{\Gamma\left[y(t)\,|\tilde{\mathbf{a}}\right]\right\}, \tag{15}$$

where the metric $\Gamma\left[y(t)\,|\tilde{\mathbf{a}}\right]$ to be maximized is given by (14).

A few remarks about the proposed detection scheme are now in order.

1) Substituting (8)-(9) into (12)-(13) and assuming high SNR, it can be found

$$q_0(t) = \frac{\left[\varphi(\tilde{\mathbf{a}}) - \eta(\tilde{\mathbf{a}})\zeta(\tilde{\mathbf{a}})\right]q(t)}{1-\eta^2(\tilde{\mathbf{a}})} + \frac{\left[\xi(\tilde{\mathbf{a}}) - \eta(\tilde{\mathbf{a}})\varphi(\tilde{\mathbf{a}})\right]g(t)}{1-\eta^2(\tilde{\mathbf{a}})}, \tag{16}$$

$$g_0(t) = \frac{\left[\varphi(\tilde{\mathbf{a}}) - \eta(\tilde{\mathbf{a}})\xi(\tilde{\mathbf{a}})\right]g(t)}{1-\eta^2(\tilde{\mathbf{a}})} + \frac{\left[\zeta(\tilde{\mathbf{a}}) - \eta(\tilde{\mathbf{a}})\varphi(\tilde{\mathbf{a}})\right]q(t)}{1-\eta^2(\tilde{\mathbf{a}})}, \tag{17}$$

where $\varphi(\tilde{\mathbf{a}}) \triangleq \frac{1}{M+1}\sum_{i=0}^{M}\prod_{k=0}^{i}\tilde{a}_k\prod_{l=0}^{i}a_l$, $\zeta(\tilde{\mathbf{a}}) \triangleq \frac{1}{M+1}\sum_{i=0}^{M}a_{i+1}\prod_{k=0}^{i}\tilde{a}_k\prod_{l=0}^{i}a_l$ and $\xi(\tilde{\mathbf{a}}) \triangleq \frac{1}{M+1}\sum_{i=0}^{M}a_i\prod_{k=0}^{i}\tilde{a}_k\prod_{l=0}^{i}a_l$. From (16)-(17), we argue that when $\tilde{\mathbf{a}} \neq \mathbf{a}$ the optimal estimates $q_0(t)$ and $g_0(t)$ differ from $q(t)$ and $g(t)$, respectively. On the other side, when $\tilde{\mathbf{a}} = \mathbf{a}$ occurs, $\varphi(\mathbf{a}) = 1$ and $\xi(\mathbf{a}) = \zeta(\mathbf{a}) = \eta(\mathbf{a})$ hold true, and therefore, $q_0(t)$ and $g_0(t)$ coincide asymptotically with the desired segments $q(t)$ and $g(t)$, provided that $\eta(\mathbf{a}) \neq 1$.

2) The occurrence of $\eta(\tilde{\mathbf{a}})$ in the objective function (14) adds to the computational complexity of the detector. A approximate yet simpler approach[1] consists in getting rid of $\eta(\tilde{\mathbf{a}})$[2]. Thus, (14) turns into

$$\bar{\Gamma}\left[y(t)\,|\tilde{\mathbf{a}}\right] = \int_0^{T_s} \left[z_1^2(t;\tilde{\mathbf{a}}) + z_2^2(t;\tilde{\mathbf{a}})\right] dt, \tag{18}$$

where $z_1(t;\tilde{\mathbf{a}})$ and $z_2(t;\tilde{\mathbf{a}})$ are given again by (8)-(9).

3) Since the information symbols take values in $\{\pm 1\}$, a further rearrangement of the metric (18) is enabled, which is particularly suitable for practical implementations of the TF-MSDD. Indeed, it is possible to show that

$$\bar{\Gamma}\left[y(t)\,|\tilde{\mathbf{a}}\right] = \sum_{i=1}^{M}\sum_{l=0}^{i-1}\prod_{k=1}^{i-l}\tilde{a}_{k+l}(Y_{l,i} + Y_{l+1,i+1}), \tag{19}$$

where the real-valued coefficients given by $Y_{i,j} \triangleq \frac{1}{M+1}\int_0^{T_s} y(t+iT_s)y(t+jT_s)dt$ are generated by correlating symbol-long segments of the received signal $y(t)$ up to M symbols away.

4) In order to maintain performance together with affordable complexity, a viable route is to take advantage of the sphere decoding (SD) method [6] and rearrange (19) into the new objective function (this time to be minimized)

$$\Phi\left[y(t)\,|\tilde{\mathbf{a}}\right] = \sum_{i=1}^{M}\sum_{l=0}^{i-1}\vartheta_{l,i}\left|Y_{l,i} + Y_{l+1,i+1}\right|, \tag{20}$$

where $\vartheta_{l,i} \triangleq 1-\sigma_{l,i}\prod_{k=1}^{i-l}\tilde{a}_{k+l}$ and $\sigma_{l,i} \triangleq \mathsf{sign}\{Y_{l,i} + Y_{l+1,i+1}\}$. Observing that (20) defines a sphere in the M-dimensional lattice of the trial vectors $\tilde{\mathbf{a}} \triangleq [\tilde{a}_1, \tilde{a}_2, \cdots, \tilde{a}_M]^T$, it can be proved that the SD-based SF-MSDD consists in examining iteratively only those lattice points (assumed to belong to a given finite-alphabet) inside a sphere of a given radius, which is progressively made smaller and smaller to reduce the search space, thereby lessening the overall computational complexity.

[1]This is motivated motivated by the assumption of independent and equally distributed information-bearing symbols

[2]We note that there will exist a (limited) percentage of symbol sequences for which $|\eta(\tilde{\mathbf{a}})| \ll 1$ will not be fulfilled at all. Therein, some form of information symbol precoding could be employed to make this condition more rigorous, although this is out of the scope of the current paper.

IV. Performance Results and Final Remarks

The BER robustness of the SF-MSDD receiver is evaluated through computer simulations for a dense-multipath single-user scenario, taking as performance benchmarks the conventional single-user Rake receiver with perfect channel state information (CSI) and ideal timing recovery (IRake), and the single-user symbol-by-symbol DD with ideal timing recovery (IDD) and without timing recovery (TF-DD).

Simulation Setup. Each active user transmits asynchronously consecutive bursts of M binary PAM symbols during which the transmission channel (assumed to be time invariant) is generated randomly according to the above propagation model [7]. The monocycle $u(t)$ has been selected as the second derivative of a Gaussian shape with normalized unit energy and pulse width equal to 1.0 ns. The frame and chip interval are $T_f = 100$ ns and $T_c = 1.0$ ns, respectively, $N_f = 10$ is the number of frames in each information symbol, the TH codes are randomly picked up in the interval $[0, 90]$, whereas the $N_u - 1$ interfering users and the desired one have power P_i and P_u, respectively, so that the nearfar ratio (NFR) results as $\text{NFR} \triangleq P_i/P_u$. Further, the timing offset of the desired user is equally distributed within the symbol interval with the exclusion of the edge intervals $[0, 0.1T_s)$ and $[0.9T_s, T_s)$, in line with the assumption that the timing information is partially acquired at symbol-level only

BER in the Single-User Scenario. Figure 1 illustrates the BER performance of the SF-MSDD in the single-user scenario ($N_u = 1$) for different block sizes, namely, $M = 5, 10, 15, 20, 30, 35$. As expected, the SF-MSDD performs better and better as the block size M increases. At BER$= 10^{-2}$, the performance gap between the $M = 5$ scheme and that with $M = 10$ is more than 6 dB, while passing to $M = 35$ offers an additional gain over $M = 10$ of 5 dB. Further, the SF-MSDD has a significant edge over the conventional IDD and TF-DD schemes, whereas it is outperformed by the IRake by approximately 10 dB, but at the price of calling for accurate channel and timing estimation.

BER in the MAI Scenario. The BER curves of Fig. 2 quantify the MAI effects on the SF-MSDD adopting as block size $M = 30$, when the number of active users is $N_u = 5, 10$, and the NFR parameter is set to -6 dB (circle marks) and -3 dB (triangle marks). With NFR = -6 dB, the SF-MSDD can sustain $N_u = 5$ users at BER = 10^{-2} with a degradation around 0.5 dB with reference to the single-user case, which raises to 1.4 dB when the MAI level raises to $N_u = 10$. Setting NFR = -3 dB, instead, the SF-MSDD with $N_u = 5$ reaches the BER level of 10^{-2} with a 4 dB loss compared with the $N_u = 1$ case, while choosing $N_u = 10$ the BER (asymptotically) increases to $5 \cdot 10^{-2}$.

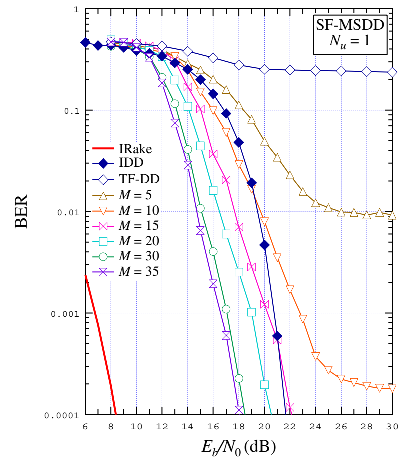

Fig. 1. BER in the single-user scenario for various M.

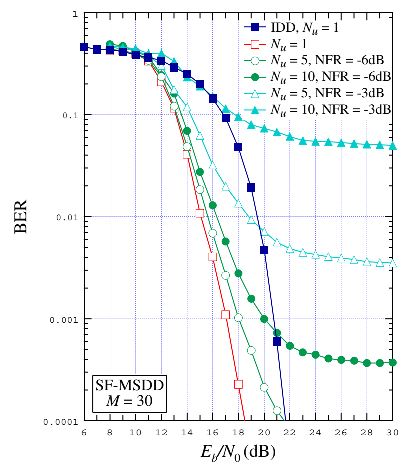

Fig. 2. BER in the multi-user scenario for various N_u.

References

[1] L. Yang and G. B. Giannakis, "Ultra-Wideband Communications: An Idea whose Time has Come," *IEEE Signal Processing Magazine*, vol. 21, no. 6, pp. 26-54, Nov. 2004.

[2] V. Lottici, A. D'Andrea and U. Mengali, "Channel Estimation for Ultra-Wideband Communications," *IEEE J. Sel. Areas Commun.*, vol. 20, no. 12, pp. 1638-1645, Dec. 2002.

[3] R. Hoctor, H. Tomlinson, "Delay-Hopped Transmitted-Reference RF Communications," *IEEE UWBST*, pp. 265-269, May 2002.

[4] M. Ho, S. Somayazulu, J. Foerster and S. Roy, "A Differential Detector for UWB Communications System," *IEEE VTC 2002*, vol. 4, pp. 1896 - 1900, May 2002.

[5] V. Lottici and Z. Tian, "Multiple Symbol Differential Detection for UWB Communications," *IEEE Trans. on Wireless Commun.*, vol. 7, no. 5, pp. 1656-1666, May 2008.

[6] U. Fincke and M. Pohst, "Improved Methods for Calculating Vectors of Short Length in a Lattice, Including a Complexity Analysis," *Math. Computation*, vol. 44, pp. 463-471, Apr. 1985.

[7] A. A. M. Saleh, and R. A. Valenzuela, "A statistical Model for Indoor Multipath Propagation," *IEEE J. Sel. Areas Commun.*, vol. 5, no. 2, pp. 128-137, Feb. 1987.